

# The effect of obliquity-driven changes on paleoclimate sensitivity during the late Pleistocene

Peter Köhler<sup>1</sup>, Gregor Knorr<sup>1</sup>, Lennert B. Stap<sup>1</sup>, Andrey Ganopolski<sup>2</sup>, Bas de Boer<sup>3</sup>, Roderik S. W. van de Wal<sup>3</sup>, Stephen Barker<sup>4</sup>, Lars H. Rüpke<sup>5</sup>

---

Peter Köhler, Peter.Koehler@awi.de

<sup>1</sup>Alfred-Wegener-Institut

Helmholtz-Zentrum für Polar-und

Meeresforschung (AWI), P.O. Box 12 01 61,

27515 Bremerhaven, Germany

<sup>2</sup>Potsdam Institute for Climate Impact

Research (PIK), Potsdam, Germany

<sup>3</sup>Institute for Marine and Atmospheric

research Utrecht (IMAU), Utrecht

University, Princetonplein 5, 3584 CC

Utrecht, The Netherlands

<sup>4</sup>School of Earth and Ocean Science,

Cardiff University, UK

This article has been accepted for publication and undergone full peer review but has not been through the copyediting, typesetting, pagination and proofreading process, which may lead to differences between this version and the Version of Record. Please cite this article as doi: 10.1029/2018GL077717

We reanalyze existing paleodata of global mean surface temperature  $\Delta T_g$  and radiative forcing  $\Delta R$  of  $\text{CO}_2$  and land ice albedo for the last 800,000 years to show that a state-dependency in paleoclimate sensitivity  $S$ , as previously suggested, is only found if  $\Delta T_g$  is based on reconstructions, and not when  $\Delta T_g$  is based on model simulations. Furthermore, during times of decreasing obliquity (periods of land-ice sheet growth and sea level fall) the multi-millennial component of reconstructed  $\Delta T_g$  diverges from  $\text{CO}_2$ , while in simulations both variables vary more synchronously, suggesting that the differences during these times are due to relatively low rates of simulated land ice growth and associated cooling. To produce a reconstruction-based extrapolation of  $S$  for the future we exclude intervals with strong  $\Delta T_g$ - $\text{CO}_2$  divergence and find that  $S$  is less state-dependent, or even constant (state-independent), yielding a mean equilibrium warming of 2–4 K for a doubling of  $\text{CO}_2$ .

**Keypoints:**

- Proxy-based reconstructions and model-based simulations of global mean surface temperature over the last 800000 years differ in detail
- During periods of decreasing obliquity and sea level the proxy reconstructions show a temperature- $\text{CO}_2$  divergence missing in simulations

<sup>5</sup>GEOMAR Helmholtz Centre for Ocean

Research Kiel, Wischhofstr. 1-3, 24159 Kiel,

Germany

- Elimination of these periods leads to a more linear paleoclimate sensitivity and to equilibrium warming for CO<sub>2</sub> doubling of 2–4 K

Accepted Article

## Plain Language Summary

Anthropogenic carbon dioxide (CO<sub>2</sub>) emissions will lead to rising global mean temperature through the greenhouse effect. The amplitude of this warming, as estimated with computer simulations for the equilibrium climate response to a doubling of atmospheric CO<sub>2</sub> concentration, is called climate sensitivity. It is necessary to verify these simulation-based quantifications of climate sensitivity with independent alternative approaches. One such approach is the analysis of past (paleo) climates, which has indicated a state-dependent paleoclimate sensitivity. Here, we compare different data-based reconstructions and computer-based simulations of paleoclimate sensitivity of the last 800,000 years and find that they disagree. In data-based reconstructions global mean temperature and CO<sub>2</sub> diverge during intervals when land ice growth is particularly pronounced. This temperature-CO<sub>2</sub> divergence is not observed in simulations, probably due to an underestimation of the rate of land ice growth and the associated cooling. However, these periods of pronounced land ice growth are not of relevance for a warming future and can therefore be neglected when estimating climate sensitivity from reconstructions of the past. Consequently, we find that paleoclimate sensitivity derived from reconstructions is less state-dependent than previously thought and agrees with warming estimates of 2–4°C as derived from simulated equilibrium climate response for CO<sub>2</sub> doubling.

### 1. Introduction

Analyses of paleo reconstructions [*Köhler et al.*, 2015] (K2015 in the following) and paleo climate simulations [*Friedrich et al.*, 2016] (F2016 in the following), covering the late Pleistocene, have suggested that climate sensitivity might not be a constant param-

eter of the climate system, but a state-dependent variable that increases towards warmer climates. Most other studies on this topic indicate a similar behavior, including a review that covers a wide range of colder and warmer climate states [von der Heydt et al., 2016]. However, there have also been studies using general circulation models (GCMs) or Earth system models of intermediate complexity (EMICs) which simulate an increase in climate sensitivity for colder than present-day climate [e.g. Colman and McAvaney, 2009; Kutzbach et al., 2013; Pfister and Stocker, 2017].

Fueled by this ambiguity we wanted to test the robustness of the conclusions in earlier studies (K2015, F2016). Here we investigate whether this, previously found, state-dependency of climate sensitivity can be reproduced in other setups, we reanalyze the proxy-based reconstructions of global temperature change ( $\Delta T_g$ ) published in the last few years [Snyder, 2016, in addition to K2015 and F2016], investigate transient 800-kyr simulation results obtained with the EMICs, CLIMBER [Ganopolski and Calov, 2011] and LOVECLIM (F2016), and analyze the only available transient GCM simulation across the last glacial/interglacial transition provided by the CCSM3 model [Liu et al., 2009; He, 2011] (Fig. 1).

A direct comparison of today's anthropogenic warming with paleodata-based reconstructions is not possible, due to the lack of a direct analog in the magnitude of the rate of changes. However, we can evaluate the general climate system response to radiative forcing anomalies. For such efforts, the specific equilibrium climate sensitivity  $S_{[X]}$  (or paleoclimate sensitivity) has been defined as the ratio of the global and annual mean surface temperature change ( $\Delta T_g$ ) over the change in radiative forcing ( $\Delta R_{[X]}$ ) caused by

the process(es) X [*PALAESENS-Project Members*, 2012]

$$S_{[X]} = \frac{\Delta T_g}{\Delta R_{[X]}} \quad (1)$$

Here, we calculate radiative forcing for processes including the greenhouse gas (GHG) effect (CO<sub>2</sub>, CH<sub>4</sub> and N<sub>2</sub>O), but also other processes, such as the (planetary) albedo effects from land ice (LI), vegetation (VG) and aerosols (AE). The time-dependency of the climate to those forcing or feedback processes is not of particular interest in the following, but has been addressed elsewhere [e.g. *Zeebe*, 2013; *Rohling et al.*, 2018]. This concept of calculating  $S_{[X]}$  was introduced in *PALAESENS-Project Members* [2012] to clarify which forcing is explicitly included when estimating climate sensitivity from paleodata, not to test causation. Furthermore, this approach assumes that different forcing processes have a similar impact on  $\Delta T_g$ , which is a simplification [e.g. *Yoshimori et al.*, 2011; *Stap et al.*, 2018], that is difficult to overcome in analyses of mainly proxy-based reconstructions. Within the context of Earth system model analysis this ratio  $\Delta T_g/\Delta R_{[X]}$  is also called the *climate sensitivity parameter* [e.g. *Yoshimori et al.*, 2011].

The emergence of state-dependency in  $S_{[X]}$  implies that the best fit to a scatter plot of  $\Delta T_g$  versus  $\Delta R_{[X]}$  is not linear, but some non-linear function, e.g. a higher order polynomial (Fig. 2a). While the detection of such a non-linearity is rather straight forward, the quantification of  $S_{[X]}$  is more complicated, as described in detail by *Köhler et al.* [2017a].

In F2016 two independent estimates of  $\Delta T_g$  were generated: a purely proxy-based reconstruction based on SST data from 63 records and a simulation with the LOVECLIM model. The estimates of  $\Delta T_g$  were then averaged and confirmed the state-dependency

in  $S_{[X]}$  for the last  $\sim 800$  kyr as deduced by K2015. Since this state-dependency in  $S_{[X]}$  suggests that during warm interglacials a relatively small change in  $\Delta R$  leads to a relatively large change in  $\Delta T_g$  (Fig. 2a), it is crucial to know how robust this conclusion is. Recently, a new proxy-based reconstruction of global mean temperature changes constructed from 61 records of SST anomalies has been published [Snyder, 2016]. These two proxy-based reconstructions of  $\Delta T_g$  [F2016, Snyder, 2016] are not fully independent with respect to the underlying data, but differ in details and in the upscaling methodologies.

Finally, we discuss how our findings for paleoclimate sensitivity can be extrapolated to the future and compare a rough approximation of equilibrium global warming caused by  $2\times\text{CO}_2$  with other approaches.

## 2. Methods

In K2015 deconvolution of the LR04 benthic  $\delta^{18}\text{O}$  stack [Lisiecki and Raymo, 2005] was used to provide mutually consistent contributions from sea level (or land ice volume) and deep ocean temperature ( $\Delta T_O$ ) using 3-D ice sheet models of *de Boer et al.* [2014]. Temperature change over land in the high latitude northern hemisphere (about  $40 - 85^\circ\text{N}$ ,  $\Delta T_{\text{NH}}$ ) where most glacial/interglacial changes in land ice occurred during the late Pleistocene, is linearly related to  $\Delta T_O$  on a multi-millennial timescale. However,  $\Delta T_{\text{NH}}$  also contains changes due to elevation changes (lapse rate) and considers seasonality.  $\Delta T_g$  and  $\Delta T_{\text{NH}}$  are then related to each other via a non-constant polar amplification factor ( $f_{\text{pa}}$ ) that has been determined from PMIP3 output. Sensitivity analyses [*de Boer et al.*, 2014, K2015] have shown that  $\Delta T_g$  has a relative uncertainty of  $\sim 10\%$  over the last 800 kyr. This setup is a model-based interpretation of proxy data. It is a mixture

between a purely proxy-based reconstruction and model-based simulations. However, while full climate models are driven by temporal changes in various boundary conditions (e.g. insolation, GHG), and then calculate all other variables internally, here only the ice sheet dynamics are simulated. Therefore, we consider our approach to be more similar to those of the proxy-based reconstructions than of the model-based simulations. From the three alternative time series, based on different assumptions for the polar amplification factor  $f_{pa}$  in K2015, we use the standard case ( $\Delta T_{g1}$ ), in which  $f_{pa}$  is linearly related to  $\Delta T_{NH}$ . However, our conclusions are not dependent on this choice of  $f_{pa}$  and  $\Delta T_g$  (see the application of the alternative temperature time series in Fig. S1). The fact that three alternative formulations of  $\Delta T_g$  can be connected to the same  $\Delta R_{[LI]}$ , shows that there are some degrees of freedom in the connection of both variables.

In K2015 the radiative forcing of CO<sub>2</sub> ( $\Delta R_{[CO_2]} = 5.35 \cdot \ln(CO_2/(278\text{ppm}))\text{W/m}^2$ , *Myhre et al.* [1998]) and land ice albedo was considered explicitly — leading to  $\Delta R_{[CO_2,LI]}$  and to the state-dependency in  $S_{[CO_2,LI]}$ . It should be noted that, when following the revised formulation of *Etminan et al.* [2016],  $\Delta R_{[CO_2]}$  differs by less than 0.01 W/m<sup>2</sup> [*Köhler et al.*, 2017b]. Furthermore, we assume that radiative forcing is state-independent, which might be a simplification [e.g. *Forster et al.*, 2016]. We will analyze similar variables based on alternative  $\Delta T_g$  from proxies (F2016, *Snyder* [2016]), and simulations (LOVECLIM (F2016), CLIMBER [*Ganopolski and Calov*, 2011], CCSM3 [*Liu et al.*, 2009; *He*, 2011]). We will first analyze these different  $\Delta T_g$  in relation to the same  $\Delta R_{[CO_2,LI]}$  as derived in K2015, but for in-depth investigations of simulations we only use the internally applied radiative forcing. The use of these alternative  $\Delta T_g$  for identical  $\Delta R_{[CO_2,LI]}$  has the poten-

tial to introduce a bias because temperature and land ice distribution are firmly linked through deconvolution of the LR04 benthic  $\delta^{18}\text{O}$  stack. This potential bias is not investigated any further here, although alternative land ice distribution [e.g. ICE-5G of *Peltier*, 2004] agree well with our results (K2015). Alternative approaches to estimate  $\Delta R_{[\text{LI}]}$  from sea level changes have shortcomings, since they omit the latitudinal effect of land ice distribution on radiative forcing (see K2015 for further details). Chronological misfits between the different records, that might also be introduced in that way, should not be of importance here, as our final interpretations are based on 8-kyr running means. Details of both alternative  $\Delta R_{[\text{LI}]}$  estimates and chronological issues have been discussed previously [K2015, *Köhler et al.*, 2017a]. For the CLIMBER simulations additional processes ( $\text{CH}_4$ ,  $\text{N}_2\text{O}$ , vegetation, aerosols) in the radiative forcing term  $\Delta R_{[\text{X}]}$  are also considered.

Time series are standardized before analysis. Due to very high variability in calculated ratios (Figs. 3b,c, S1b,c) data far away from the mean ( $|\Delta T_g/\Delta R_{[\text{CO}_2, \text{LI}]}| > 0.25\sigma$ ;  $|\Delta R_{[\text{LI}]}/\Delta R_{[\text{CO}_2]}| > 1\sigma$ ) are considered as outliers and removed. The chosen cut-off thresholds mainly influence the peak height in the standardized time series, but not the dynamics contained in the time series. Due to the rather linear behaviour of the simulations, no outliers in  $\Delta T_g/\Delta R_{[\text{CO}_2, \text{LI}]}$  have been removed from the LOVECLIM and CLIMBER results. Finally, the outlier-free time series are standardized a second time to enable comparison between the different approaches. This outlier selection during standardization is illustrated for K2015 in Fig. S2.

The land ice dynamics simulated in CLIMBER (which are also used in LOVECLIM via offline coupling) are restricted to northern hemisphere ice sheets, Antarctic land ice is

kept fixed at present day configuration, while in K2015 the dynamics of ice sheets and ice shelves in both hemispheres have been investigated. The CCSM3 simulations [*Liu et al.*, 2009; *He*, 2011] were driven by the ICE-5G land ice distribution, which was compared to *de Boer et al.* [2014] in K2015. This ICE-5G-based  $\Delta R_{[LI]}$  is also used here when investigating CCSM3 results.

We use the internal fitting routines of the software package GLE, the Graphics Layout Engine (<http://www.gle-graphics.org>) and use  $F$ -tests to determine whether a second order polynomial fits the scattered  $\Delta T_g$ - $\Delta R$ -data better than a linear approach (Table S1). For all fits the pre-condition of meeting the origin is applied (no temperature change for no forcing change), leading to the following two regression equations to be tested: either  $y = b \cdot x$  (linear) or  $y = b \cdot x + c \cdot x^2$  (non-linear).

In cases where uncertainties in both  $\Delta T_g$  and  $\Delta R_{[X]}$  are available, more elaborate statistics might be applied (e.g. Monte-Carlo approaches have been used in K2015). Uncertainties in  $\Delta T_g$  are only available for K2015 and Snyder. In Fig. S3, we show that non-linear fits are very similar when considering or ignoring uncertainties in these two data sets.

We take this as support for the more simplistic approach in our main analysis: all data sets are treated identically and fits are calculated without considering uncertainties in the scattered data.

### **3. Results and Discussions**

#### **3.1. Proxy-based reconstructions versus model-based simulations**

The main difference between proxy-based reconstructions and model-based simulations to estimate global temperature changes, is that the proxy-based reconstructions capture

the impacts of all Earth system processes active in the considered time window, while in the model-based approaches only those processes implemented in the model can leave their imprint in the simulation results. Simulated time series of  $\Delta T_g$ , therefore, have to be questioned critically for any serious omissions. In other words, any persisting difference between proxy-based reconstructions and simulated  $\Delta T_g$  might be caused by those processes not included in the models. Alternatively, proxy-based reconstructions might be systematically biased, although this seems unlikely if independent reconstructions come to similar conclusions.

Here we compare results of others to the approach of K2015 (Fig. 1a) in order to understand when the proposed state-dependency in  $S_{[\text{CO}_2, \text{LI}]}$  is sustained or when it needs to be rejected. If we replace  $\Delta T_g$  with an alternative time series (F2016, Snyder, CLIMBER, LOVECLIM, CCSM3, Fig. 1b,c), we find a similar state-dependency in  $S_{[\text{CO}_2, \text{LI}]}$  — with higher values for warmer conditions — when the applied  $\Delta T_g$  time series is based on proxy-based reconstructions (Fig 2b). This holds for the temperature data set of Snyder, as well as for proxy-based  $\Delta T_g$  derived in F2016 (Fig 2b). The non-linearity in the  $\Delta T_g$ - $\Delta R_{[\text{CO}_2, \text{LI}]}$  scatter plots is less pronounced in these alternative calculations, when compared to K2015.

If temperature anomalies are taken from CLIMBER simulations, a non-linear relationship between  $\Delta T_g$  and  $\Delta R_{[\text{CO}_2, \text{LI}]}$  is generated that is inverse to that found by K2015 (Fig. 2c), suggesting a smaller paleoclimate sensitivity for warmer climates. Similarly, if we base this analysis on the  $\Delta T_g$  simulated in LOVECLIM, we find an inverse non-linear relationship — opposite to the proxy-based results (Fig 2c). Since the  $\Delta T_g$ - $\Delta R_{[\text{CO}_2, \text{LI}]}$

relationship of the proxy-based reconstructions of F2016 and the transient LOVECLIM simulations show the opposite slope, it is natural that an averaged  $\Delta T_g$  based on both (as used in F2016) contains a rather linear relationship (Fig. 2d). Finally we analyzed the only available transient GCM-simulation, the Trace21K scenario of the CCSM3 model for the last 21 kyr. Using their  $\Delta T_g$ , we again find the same results as from the EMIC runs (Fig. 2d) — a state-dependent paleoclimate sensitivity with steeper slopes in the  $\Delta T_g$ - $\Delta R_{[\text{CO}_2, \text{LI}]}$  data during colder climates, pointing to a higher  $S_{[\text{CO}_2, \text{LI}]}$ , which is inverse to the results from the proxy-based approaches.

If we analyze internally consistent EMIC simulation results using the radiative forcing of  $\text{CO}_2$  and land ice applied in the model runs together with the simulated  $\Delta T_g$  (instead of  $\Delta R_{[\text{CO}_2, \text{LI}]}$  based on K2015), we find a linear relationship between  $\Delta T_g$  and  $\Delta R_{[\text{CO}_2, \text{LI}]}$  for LOVECLIM (Fig. 2e). In CLIMBER we find a similar non-linear relationship between  $\Delta T_g$  and  $\Delta R_{[\text{CO}_2, \text{LI}]}$  — with steeper slope during cold climate— as in the approaches in which the CLIMBER-simulated  $\Delta T_g$  was analyzed together with  $\Delta R_{[\text{CO}_2, \text{LI}]}$  of K2015 (Fig. 2e). Further details on the differences in  $\Delta R_{[\text{LI}]}$  for the different approaches can be found in Fig. S4.

### 3.2. Obliquity-driven changes and the $\Delta T_g$ – $\text{CO}_2$ relationship

How can we understand this strong state-dependency of  $S$  found in proxy-based approaches and the difference to the model-based approaches? It has recently been deduced, from ice core data covering the last 800 kyr, that the multi-millennial trend of atmospheric  $\text{CO}_2$  concentration and Antarctic temperature diverge when obliquity decreases [*Hasen-clever et al.*, 2017]. One way of perceiving this divergence is that the reduced incoming

insolation at high latitudes causes land ice sheet growth and cooling, while there is a coexisting process that keeps CO<sub>2</sub> at a relatively constant level. Solid Earth modeling experiments have indicated that falling sea level might lead to enhanced magma and CO<sub>2</sub> production at mid ocean ridges [e.g. *Lund and Asimow, 2011*]. *Hasenclaver et al.* [2017] suggested, that the combination of marine volcanism at mid ocean ridges and at hotspot island volcanoes might react to decreasing sea level and be a potential cause for this  $\Delta T_g$ -CO<sub>2</sub> divergence. Alternatively, the divergence implies that processes other than CO<sub>2</sub> radiative forcing or land ice albedo (potentially radiative forcing from non-CO<sub>2</sub> GHGs, or albedo change caused by aerosols, or vegetation) dominate during these phases — leading to a cooling with little reduction in CO<sub>2</sub>. The evidence so far [e.g. *Köhler et al., 2010*] does not indicate that the latter was the case, although potential impacts of different forcing efficacy [e.g. *Yoshimori et al., 2011*; *Stap et al., 2018*] have so far not been investigated. One study analyzed the contribution of the terrestrial carbon cycle to the divergence of CO<sub>2</sub> and  $\Delta T_g$  at the end of the present (Holocene) and the previous (Eemian or MIS 5e) interglacial [*Brovkin et al., 2016*]. Processes which seemed to explain the reconstructed divergence in the Holocene failed to explain similar dynamics during MIS 5e, pointing to model deficiencies in the representation of the land carbon cycle, or suggesting that other processes are at work. All modeling results used in here (CLIMBER, LOVECLIM, CCSM3) were obtained in simulations with prescribed observed CO<sub>2</sub> concentrations, and thus include all effects of the Earth system feedbacks on CO<sub>2</sub>. However, simulation results do not contain the characteristic long-term  $\Delta T_g$ -CO<sub>2</sub> divergence found in the proxy-based reconstructions (*Snyder, F2016*), or in the deconvolution of LR04- $\delta^{18}O$

into land ice dynamics (K2015). This suggests that a relatively low rate of simulated land ice growth and associated cooling during times of decreasing obliquity, and not a feedback on CO<sub>2</sub>, might be responsible for the difference between model- and proxy-based approaches.

When  $\Delta T_g$  is derived mainly from proxy-based reconstructions (K2015, F2016, Snyder), our results show a strong  $\Delta T_g$ -CO<sub>2</sub> divergence at times of obliquity decrease. An example of this is the dynamics at the end of the Eemian (see zoom-in in the inset in Fig. 1a). For comparison of the different approaches, all time series in the following are analyzed in their standardized versions (Fig. 3, Fig. S1). They confirm the earlier finding of a temperature-CO<sub>2</sub> divergence at times of obliquity decrease by *Hasenclever et al.* [2017], in which not global temperature change, but Antarctic temperature change derived from the EPICA Dome C (EDC) ice core [Jouzel et al., 2007] has been considered. The temporal evolution of this divergence between  $\Delta T_g$  and CO<sub>2</sub> can be observed by analyzing the multi-millennial dynamics of the ratio  $\Delta T_g/\Delta R_{[CO_2]}$ , which by coincidence is also defined as  $S_{[CO_2]}$  (Fig. 3b). The interpretation of  $S_{[CO_2]}$  as a proxy for the multi-millennial  $\Delta T_g$ -CO<sub>2</sub>-divergence represents a major improvement in the understanding of  $S_{[CO_2]}$ , since previously no meaningful patterns have been detected in its temporal variability [PALAEOSENS-Project Members, 2012]. We find that a strong  $\Delta T_g$ -CO<sub>2</sub> divergence exists in 12 out of 19 phases with decreasing obliquity (gray bands in Fig. 3) in the data from K2015. Furthermore, the ratio of land ice and CO<sub>2</sub> radiative forcing ( $\Delta R_{[LI]}/\Delta R_{[CO_2]}$ ) underwent large changes during these intervals (Fig. 3c), suggesting that land ice (sea level) related changes might indeed be connected to the times of these diverging trends.

The seven phases with decreasing obliquity, but without strong  $\Delta T_g$ -CO<sub>2</sub> divergence in K2015, can furthermore be divided into periods with a stable ratio of  $\Delta R_{[LI]}/\Delta R_{[CO_2]}$  (light blue bands marked A, D, G, P) and those with strong variability in  $\Delta R_{[LI]}/\Delta R_{[CO_2]}$  (light red bands I, K, R). In the former periods (blue-colored) the stable ratio of land ice and CO<sub>2</sub> radiative forcing suggests in-phase variations of both processes, which might indicate that any potential sea level-related CO<sub>2</sub> outgassing from marine volcanism or other processes could be compensated by the land ice sheet albedo feedback. In the latter periods (red-colored) the ratio  $\Delta T_g/\Delta R_{[CO_2]}$  is always increasing towards the end of the obliquity-half cycle, suggesting that some sea level-related process affecting CO<sub>2</sub> might have initiated, but not yet developed its full potential. This leads, for example, to the unusual strong  $\Delta T_g$ -CO<sub>2</sub> divergence after the end of period K at 436 kyr BP which persisted for almost a complete obliquity cycle around MIS 11. Five of these seven phases with decreasing obliquity but without a strong  $\Delta T_g$ -CO<sub>2</sub> divergence (A, D, I, K, P, but not G and R) are also characterized by very modest cooling, indicating that the net climate changes during these phases are small when compared to other phases with decreasing obliquity. These phases should, therefore, be interpreted with care since the dominant climate variations occur during other times.

Much smaller variations in the  $\Delta T_g$ -CO<sub>2</sub> divergence are found when analyzing model-based simulations of CLIMBER and LOVECLIM than in K2015 (Fig. 3b). Furthermore, the model-based  $\Delta T_g$ -CO<sub>2</sub> divergence observed during times of decreasing obliquity is partially in anti-phase to the proxy-based results (phases C, S), suggesting highly synchronous variations in CO<sub>2</sub> and simulated  $\Delta T_g$  while a strong divergence to CO<sub>2</sub> persists

in the reconstructed  $\Delta T_g$  (Fig. 3b). The two lukewarm interglacials MIS 15a, and 15e (phases N, O, 570 and 610 kyr BP, respectively, [*Past Interglacials Working Group of PAGES*, 2016]) seem to be special in this respect, since the  $\Delta T_g$ -CO<sub>2</sub> divergence from K2015 is in anti-phase to those based on the simulation output and also to that based on EDC  $\Delta T$ . Interestingly, the temperature-CO<sub>2</sub> divergence during the MIS 5/4 transition, around 75 kyr BP (phase B) which motivated the study of *Hasenclever et al.* [2017], is one of the largest in EDC, but rather weak in K2015. Our calculated  $\Delta T_g$ -CO<sub>2</sub> divergence, based on  $\Delta T_g$  of Snyder or F2016, contains qualitatively similar dynamics related to obliquity as that based on EDC  $\Delta T$  or K2015, but differs from the model-based simulations (Fig. S1). This qualitative agreement of the divergence in proxy-based  $\Delta T_g$  (K2015, F2016, Snyder, EDC) provides confidence in the global temperature record obtained in K2015. Furthermore, tests have shown that if new insights into polar amplification [*Stap et al.*, 2018] are used for an improvement of the model setup used in K2015, only small changes in  $\Delta T_g$  are generated, but the general difference to the model-based simulations persists. Based on these findings, the analysis of *Hasenclever et al.* [2017] needs to be expanded: decreasing obliquity seems to be a necessary, but not a sufficient condition for the  $\Delta T_g$ -CO<sub>2</sub> divergence. Another process related to sea level change, or in detail to  $\Delta R_{[LI]}/\Delta R_{[CO_2]}$ , needs to be active at the same time to explain the data.

The importance of this  $\Delta T_g$ -CO<sub>2</sub> divergence and its connection to obliquity, for the state-dependency of our paleoclimate sensitivity estimate, becomes apparent when we split the data into times with increasing or decreasing obliquity. In the latter case the non-linearity (parameter  $c$  in the second order fit) between  $\Delta T_g$  and  $\Delta R$  is significantly

different in the data set of K2015 and Snyder (Fig. S5a,c), while in the CLIMBER output hardly any difference can be detected (Fig. S5b). For F2016 (Fig. S5d), which shows a non-linear relationship when all data are analyzed, the relationship is only linear in both data subsets when differentiated by their phase of obliquity. When data are split based on the ratio  $\Delta T_g/\Delta R_{[\text{CO}_2]}$  in subsets with strong or weak  $\Delta T_g$ -CO<sub>2</sub> divergence, we find an even larger difference in the non-linearity than when data are split by obliquity in K2015 (Fig. 2f), implying a more linear relationship for data with strong  $\Delta T_g$ -CO<sub>2</sub> divergence than for data with decreasing obliquity. When using  $\Delta T_g$  from the proxy-based reconstructions of Snyder and F2016, we find a non-linear relationship in the  $\Delta T_g$ - $\Delta R_{[\text{CO}_2,\text{LI}]}$  scatter plot during strong  $\Delta T_g$ -CO<sub>2</sub> divergence, while for times with more synchronous changes in  $\Delta T_g$  and CO<sub>2</sub> (weak divergence) a linear relationship between  $\Delta T_g$  and  $\Delta R_{[\text{CO}_2,\text{LI}]}$  emerges (Fig. 2g,h).

### 3.3. Using paleoclimate sensitivity to estimate $\Delta T_{2\times\text{CO}_2}$

The  $\Delta T_g$ -CO<sub>2</sub> divergence appears mainly during, or in connection with, periods of decreasing obliquity related to land ice growth or sea level fall. These times cover  $\sim 50\%$  of past climates. We conclude, that for a generic climate system understanding the implementation of the processes responsible for this  $\Delta T_g$ -CO<sub>2</sub> divergence, potentially being the solid Earth-climate feedbacks related to a sea level induced change in marine volcanism [e.g. *Lund and Asimow, 2011; Hasenclever et al., 2017*], is essential.

Intervals of strong  $\Delta T_g$ -CO<sub>2</sub> divergence should not be considered for the interpretation of paleodata in the context of future warming, e.g. by calculating the paleoclimate sensitivity  $S$ , because in the future we expect sea level to rise. Otherwise the climate system response

of a glaciation is erroneously implicated with anthropogenic warming. Here, one might rely only on the subset of  $\Delta T_g$ - $\Delta R$ -data that coincide with times of weak (or no)  $\Delta T_g$ - $\text{CO}_2$  divergence. For K2015, this restriction would lead to a different quantification of paleoclimate sensitivity following the framework of Köhler *et al.* [2017a] (Fig. 2f). In detail,  $S_{[\text{CO}_2, \text{LI}]}$  can be derived from the fit to the scattered  $\Delta T_g - \Delta R_{[\text{CO}_2, \text{LI}]}$  data after  $S_{[\text{CO}_2, \text{LI}]} = b + c \cdot \Delta R_{[\text{CO}_2, \text{LI}]}$ . The paleodata of the last 800 kyr cover mainly intervals with  $\Delta R_{[\text{CO}_2, \text{LI}]} \leq 0 \text{ W/m}^2$ , and due to the state-dependent character of  $S_{[\text{CO}_2, \text{LI}]}$  we refrain from an extrapolation of our derived fitting function to a range not covered by the data, e.g. to  $\Delta R_{[\text{CO}_2, \text{LI}]} > 0 \text{ W/m}^2$ . Nevertheless, climates comparable to late Pleistocene interglacials can be approximated by  $\Delta R_{[\text{CO}_2, \text{LI}]} \approx 0 \text{ W/m}^2$ .  $S_{[\text{CO}_2, \text{LI}]}$  for those interglacials would be  $\sim 20\%$  smaller when excluding intervals of  $\Delta T_g$ - $\text{CO}_2$  divergence in comparison to calculations based on all available data,  $S_{[\text{CO}_2, \text{LI}]} = 1.6 \text{ K}/(\text{W/m}^2)$  instead of  $2.0 \text{ K}/(\text{W/m}^2)$ . If based on  $\Delta T_g$  of Snyder (Fig. 2g) or F2016 (Fig. 2h) these subsets of data with weak (or no)  $\Delta T_g$ - $\text{CO}_2$  divergence are defined by a linear relationship between  $\Delta T_g$  and  $\Delta R_{[\text{CO}_2, \text{LI}]}$  and a constant  $S_{[\text{CO}_2, \text{LI}]}$  of  $0.82$  and  $0.88 \text{ K}/(\text{W/m}^2)$ , respectively. To estimate equilibrium warming caused by  $2 \times \text{CO}_2$  ( $\Delta T_{2 \times \text{CO}_2}$ , the classical Charney equilibrium climate sensitivity (ECS) [Charney *et al.*, 1979; Knutti *et al.*, 2017]) from our  $S_{[\text{CO}_2, \text{LI}]}$  we need to correct for missing slow processes (radiative forcing of  $\text{CH}_4$  and  $\text{N}_2\text{O}$ ; albedo changes caused by vegetation and aerosols). In a previous study [PALAEOSENS-Project Members, 2012] the ratio between  $S_{[\text{GHG, LI, VG, AE}]} / S_{[\text{CO}_2, \text{LI}]}$  for the last 800 kyr has been determined as  $0.64 \pm 0.07 (1\sigma)$ . Note, that this correction for the slow processes ignores any state-dependency that might be associated with them. Together with the average radiative

forcing for a doubling of CO<sub>2</sub> of 3.71 W/m<sup>2</sup> ( $\pm 10\%$  ( $1\sigma$ )) [Myhre *et al.*, 1998] our  $S_{[\text{CO}_2, \text{LI}]}$  for late Pleistocene interglacials translates into a  $\Delta T_{2\times\text{CO}_2}$  or ECS of  $1.9 \pm 0.3$  K (Snyder),  $2.1 \pm 0.3$  K (F2016) and  $3.8 \pm 0.6$  K (K2015). Alternative calculations, based on the data split by obliquity (Fig. S5), would lead to slightly larger numbers of ECS ( $2.3 \pm 0.3$  K (Snyder),  $2.3 \pm 0.3$  K (F2016) and  $4.4 \pm 0.7$  K (K2015)), however we consider these to be less reliable following our analysis in the previous subsection. This compares well with other approaches [Knutti *et al.*, 2017], including the narrow “likely” (66% confidence interval) range of 2.2–3.4 K recently obtained from an emerging constraint from global temperature variability and CMIP5 [Cox *et al.*, 2018], and the 95% confidence range of 2.0–4.3 K from a large model ensemble, which has been constrained by observational and geological evidences [Goodwin *et al.*, 2018].

#### 4. Conclusions

In conclusion, we find an inconsistency in the state-dependency of paleoclimate sensitivity calculated from model simulations and proxy-reconstructions, when explicitly considering radiative forcing of CO<sub>2</sub> change and land ice albedo change, or  $S_{[\text{CO}_2, \text{LI}]}$ . This may be related to the fact that fast climate feedbacks in EMICs are too linear. Furthermore, EMICs may underestimate the strength of some slow climate feedbacks. As it has been shown that solid Earth-climate feedbacks can play an important role for CO<sub>2</sub> dynamics during glacial cycles [e.g. Huybers and Langmuir, 2009; Lund and Asimow, 2011; Hasenlever *et al.*, 2017], these feedbacks should be incorporated in models used to simulate CO<sub>2</sub> concentration [e.g. Ganopolski and Brovkin, 2017]. Furthermore, one also needs to fully understand why current model simulations contain none of the temperature-CO<sub>2</sub>

divergence observed during intervals of decreasing obliquity within proxy-based reconstructions. Our study suggests that one possible reason for this discrepancy is that the CLIMBER model underestimates the rate of land ice growth during periods of decreasing obliquity, and consequently simulates less cooling induced by land ice. It should be emphasized that the magnitude of the expected CO<sub>2</sub> changes connected with these solid Earth feedbacks are small when compared with anthropogenic CO<sub>2</sub> changes. Therefore, these missing model feedbacks in CLIMBER do not affect its ability to simulate future temperature increase caused by a rise in CO<sub>2</sub>. Our results have important consequences for future efforts to quantify paleoclimate sensitivity from proxy-based analyses. We suggest that studies should focus on intervals without decreasing obliquity or sea level, since the detected divergence of global temperature and CO<sub>2</sub> during these intervals could otherwise overprint the system response.

### **Acknowledgments**

This is work institutional-funded at AWI via the research program PACES-II of the Helmholtz Association. It contributes to PALMOD, the German Paleomodeling Research Project funded by BMBF. B de Boer receives funding from the Veni program of the Dutch Science Foundation. This work contributes to the Netherlands Earth System Science Centre (NESSC). We thank Tobias Friedrich for providing data and Emma Smith for language editing. No new data have been generated for this work. All analyzed data sets have been taken from the cited literature.

## References

- Bazin, L., A. Landais, B. Lemieux-Dudon, H. Toyé Mahamadou Kele, D. Veres, F. Parrenin, P. Martinerie, C. Ritz, E. Capron, V. Lipenkov, M.-F. Loutre, D. Raynaud, B. Vinther, A. Svensson, S. O. Rasmussen, M. Severi, T. Blunier, M. Leuenberger, H. Fischer, V. Masson-Delmotte, J. Chappellaz, and E. Wolff (2013), An optimized multi-proxy, multi-site Antarctic ice and gas orbital chronology (AICC2012): 120–800 ka, *Climate of the Past*, *9*(4), 1715–1731, doi:10.5194/cp-9-1715-2013.
- Bereiter, B., S. Eggleston, J. Schmitt, C. Nehrbass-Ahles, T. F. Stocker, H. Fischer, S. Kipfstuhl, and J. Chappellaz (2015), Revision of the EPICA Dome C CO<sub>2</sub> record from 800 to 600 kyr before present, *Geophysical Research Letters*, *42*(2), 542–549, doi:10.1002/2014GL061957.
- Brovkin, V., T. Brcher, T. Kleinen, S. Zaehle, F. Joos, R. Roth, R. Spahni, J. Schmitt, H. Fischer, M. Leuenberger, E. J. Stone, A. Ridgwell, J. Chappellaz, N. Kehrwald, C. Barbante, T. Blunier, and D. D. Jensen (2016), Comparative carbon cycle dynamics of the present and last interglacial, *Quaternary Science Reviews*, *137*, 15 – 32, doi:<http://dx.doi.org/10.1016/j.quascirev.2016.01.028>.
- Charney, J. G., A. Arakawa, D. J. Baker, B. Bolin, R. E. Dickinson, R. M. Goody, C. E. Leith, H. M. Stommel, and C. I. Wunsch (1979), *Carbon Dioxide and Climate: A Scientific Assessment*, 33 pp., National Academy of Science, Washington, D.C.
- Colman, R., and B. McAvaney (2009), Climate feedbacks under a very broad range of forcing, *Geophysical Research Letters*, *36*, L01702, doi:10.1029/2008GL036268.

Cox, P. M., C. Huntingford, and M. S. Williamson (2018), Emergent constraint on equilibrium climate sensitivity from global temperature variability, *Nature*, *553*, 319–322, doi:10.1038/nature25450.

de Boer, B., L. J. Lourens, and R. S. van de Wal (2014), Persistent 400,000-year variability of Antarctic ice volume and the carbon cycle is revealed throughout the Plio-Pleistocene, *Nature Communications*, *5*, 2999, doi:10.1038/ncomms3999.

Etminan, M., G. Myhre, E. J. Highwood, and K. P. Shine (2016), Radiative forcing of carbon dioxide, methane, and nitrous oxide: A significant revision of the methane radiative forcing, *Geophysical Research Letters*, *43*(24), 12,614–12,623, doi:10.1002/2016GL071930.

Forster, P. M., T. Richardson, A. C. Maycock, C. J. Smith, B. H. Samset, G. Myhre, T. Andrews, R. Pincus, and M. Schulz (2016), Recommendations for diagnosing effective radiative forcing from climate models for CMIP6, *Journal of Geophysical Research: Atmospheres*, *121*(20), 12,460–12,475, doi:10.1002/2016JD025320.

Friedrich, T., A. Timmermann, M. Tigchelaar, O. Elison Timm, and A. Ganopolski (2016), Nonlinear climate sensitivity and its implications for future greenhouse warming, *Science Advances*, *2*(11), doi:10.1126/sciadv.1501923.

Ganopolski, A., and V. Brovkin (2017), Simulation of climate, ice sheets and CO<sub>2</sub> evolution during the last four glacial cycles with an Earth system model of intermediate complexity, *Climate of the Past*, *13*(12), 1695–1716, doi:10.5194/cp-13-1695-2017.

Ganopolski, A., and R. Calov (2011), The role of orbital forcing, carbon dioxide and regolith in 100 kyr glacial cycles, *Climate of the Past*, *7*(4), 1415–1425, doi:10.5194/cp-

7-1415-2011.

Goodwin, P., A. Katavouta, V. M. Roussenov, G. L. Foster, E. J. Rohling, and R. G. Williams (2018), Pathways to 1.5 °C and 2 °C warming based on observational and geological constraints, *Nature Geoscience*, *11*(2), 102–107, doi:10.1038/s41561-017-0054-8.

Hasencllever, J., G. Knorr, L. Rüpke, P. Köhler, J. Morgan, K. Garofalo, S. Barker, G. Lohmann, and I. Hall (2017), Sea level fall during glaciation stabilized atmospheric CO<sub>2</sub> by enhanced volcanic degassing, *Nature Communications*, *8*, 15867, doi: 10.1038/ncomms15867.

He, F. (2011), Simulating transient climate evolution of the last deglaciation with CCSM3, Ph.D. thesis, University of Wisconsin-Madison.

Huybers, P., and C. Langmuir (2009), Feedback between deglaciation and volcanism, and atmospheric CO<sub>2</sub>, *Earth and Planetary Science Letters*, *286*, 479–491, doi: 10.1016/j.epsl.2009.07.014.

Jouzel, J., V. Masson-Delmotte, O. Cattani, G. Dreyfus, S. Falourd, G. Hoffmann, B. Minster, J. Nouet, J. M. Barnola, J. Chappellaz, H. Fischer, J. C. Gallet, S. Johnsen, M. Leuenberger, L. Loulergue, D. Luethi, H. Oerter, F. Parrenin, G. Raisbeck, D. Raynaud, A. Schilt, J. Schwander, E. Selmo, R. Souchez, R. Spahni, B. Stauffer, J. P. Steffensen, B. Stenni, T. F. Stocker, J. L. Tison, M. Werner, and E. W. Wolff (2007), Orbital and millennial Antarctic climate variability over the last 800 000 years, *Science*, *317*, 793–796, doi:10.1126/science.1141038.

Knutti, R., M. A. A. Rugenstein, and G. C. Hegerl (2017), Beyond equilibrium climate sensitivity, *Nature Geoscience*, *10*(10), 727–736, doi:10.1038/ngeo3017.

Köhler, P., R. Bintanja, H. Fischer, F. Joos, R. Knutti, G. Lohmann, and V. Masson-Delmotte (2010), What caused Earth's temperature variations during the last 800,000 years? Data-based evidences on radiative forcing and constraints on climate sensitivity, *Quaternary Science Reviews*, *29*, 129–145, doi:10.1016/j.quascirev.2009.09.026.

Köhler, P., B. de Boer, A. S. von der Heydt, L. S. Stap, and R. S. W. van de Wal (2015), On the state dependency of equilibrium climate sensitivity during the last 5 million years, *Climate of the Past*, *11*, 1801–1823, doi:10.5194/cp-11-1801-2015.

Köhler, P., L. S. Stap, A. S. von der Heydt, B. de Boer, R. S. W. van de Wal, and J. Bloch-Johnson (2017a), A state-dependent quantification of climate sensitivity based on paleo data of the last 2.1 million years, *Paleoceanography*, *32*, 1102–1114, doi:10.1002/2017PA003190.

Köhler, P., C. Nehrbass-Ahles, J. Schmitt, T. F. Stocker, and H. Fischer (2017b), A 156 kyr smoothed history of the atmospheric greenhouse gases CO<sub>2</sub>, CH<sub>4</sub>, and N<sub>2</sub>O and their radiative forcing, *Earth System Science Data*, *9*, 363–387, doi:10.5194/essd-9-363-2017.

Kutzbach, J. E., F. He, S. J. Vavrus, and W. F. Ruddiman (2013), The dependence of equilibrium climate sensitivity on climate state: Applications to studies of climates colder than present, *Geophysical Research Letters*, *40*(14), 3721–3726, doi:10.1002/grl.50724.

Laskar, J., P. Robutel, F. Joutel, M. Gastineau, A. C. M. Correia, and B. Levrard (2004), A long term numerical solution for the insolation quantities of the Earth, *Astronomy and Astrophysics*, *428*, 261–285, doi:10.1051/0004-6361:20041335.

Lisiecki, L. E., and M. E. Raymo (2005), A Pliocene-Pleistocene stack of 57 globally distributed benthic  $\delta^{18}\text{O}$  records, *Paleoceanography*, *20*, PA1003, doi:

10.1029/2004PA001071.

Liu, Z., B. L. Otto-Bliesner, F. He, E. C. Brady, R. Tomas, P. U. Clark, A. E. Carlson, J. Lynch-Stieglitz, W. Curry, E. Brook, D. Erickson, R. Jacob, J. Kutzbach, and J. Cheng (2009), Transient Simulation of Last Deglaciation with a New Mechanism for Bølling-Allerød Warming, *Science*, *325*(5938), 310–314, doi:10.1126/science.1171041.

Lund, D. C., and P. D. Asimow (2011), Does sea level influence mid-ocean ridge magmatism on Milankovitch timescales?, *Geochemistry, Geophysics, Geosystems*, *12*, Q12009, doi:10.1029/2011GC003693.

Myhre, G., E. J. Highwood, K. P. Shine, and F. Stordal (1998), New estimates of radiative forcing due to well mixed greenhouse gases, *Geophysical Research Letters*, *25*, 2715–2718, doi:10.1029/98GL01908.

PALAEOSSENS-Project Members (2012), Making sense of palaeoclimate sensitivity, *Nature*, *491*, 683–691, doi:10.1038/nature11574.

Past Interglacials Working Group of PAGES (2016), Interglacials of the last 800,000 years, *Reviews of Geophysics*, *54*(1), 162–219, doi:10.1002/2015RG000482.

Peltier, W. R. (2004), Global glacial isostasy and the surface of the ice-age Earth: the ICE-5G (VM2) model and GRACE, *Annual Review in Earth and Planetary Sciences*, *32*, 111–149, doi:10.1146/annurev.earth.32.082503.144359.

Pfister, P. L., and T. F. Stocker (2017), State-Dependence of the Climate Sensitivity in Earth System Models of Intermediate Complexity, *Geophysical Research Letters*, *44*(20), 10,643–10,653, doi:10.1002/2017GL075457.

Rohling, E. J., G. Marino, G. L. Foster, P. Goodwin, A. von der Heydt, and P. Köhler (2018), Comparing climate sensitivity, past and present, *Annual Review of Marine Science*, 10, 261–288, doi:10.1146/annurev-marine-121916-063242.

Snyder, C. W. (2016), Evolution of global temperature over the past two million years, *Nature*, 538(7624), 226–228, doi:10.1038/nature19798.

Stap, L. B., R. S. W. van de Wal, B. de Boer, P. Köhler, J. H. Hoencamp, G. Lohmann, E. Tuenter, and L. J. Lourens (2018), The influence of land ice and CO<sub>2</sub> on polar amplification and specific equilibrium climate sensitivity during the past 5 million years, *Paleoceanography and Paleoclimatology*., doi:10.1002/2017PA003313.

Veres, D., L. Bazin, A. Landais, H. Toyé Mahamadou Kele, B. Lemieux-Dudon, F. Parrenin, P. Martinerie, E. Blayo, T. Blunier, E. Capron, J. Chappellaz, S. O. Rasmussen, M. Severi, A. Svensson, B. Vinther, and E. W. Wolff (2013), The Antarctic ice core chronology (AICC2012): an optimized multi-parameter and multi-site dating approach for the last 120 thousand years, *Climate of the Past*, 9(4), 1733–1748, doi:10.5194/cp-9-1733-2013.

von der Heydt, A. S., H. A. Dijkstra, R. S. W. van de Wal, R. Caballero, M. Crucifix, G. L. Foster, M. Huber, P. Köhler, E. Rohling, P. J. Valdes, P. Ashwin, S. Bathiany, T. Berends, L. van Bree, P. Ditlevsen, M. Ghil, A. Haywood, J. Katzav, G. Lohmann, J. Lohmann, V. Lucarini, A. Marzocchi, H. Pälike, I. R. Baroni, D. Simon, A. Sluijs, L. B. Stap, A. Tantet, J. Viebahn, and M. Ziegler (2016), Lessons on climate sensitivity from past climate changes, *Current Climate Change Reports*, 2, 148–158, doi:10.1007/s40641-016-0049-3.

Yoshimori, M., J. C. Hargreaves, J. D. Annan, T. Yokohata, and A. Abe-Ouchi (2011), Dependency of Feedbacks on Forcing and Climate State in Physics Parameter Ensembles, *Journal of Climate*, *24*(24), 6440–6455, doi:10.1175/2011JCLI3954.1.

Zeebe, R. E. (2013), Time-dependent climate sensitivity and the legacy of anthropogenic greenhouse gas emissions, *Proceedings of the National Academy of Sciences*, *110*(34), 13739–13744, doi:10.1073/pnas.1222843110.

Accepted Article

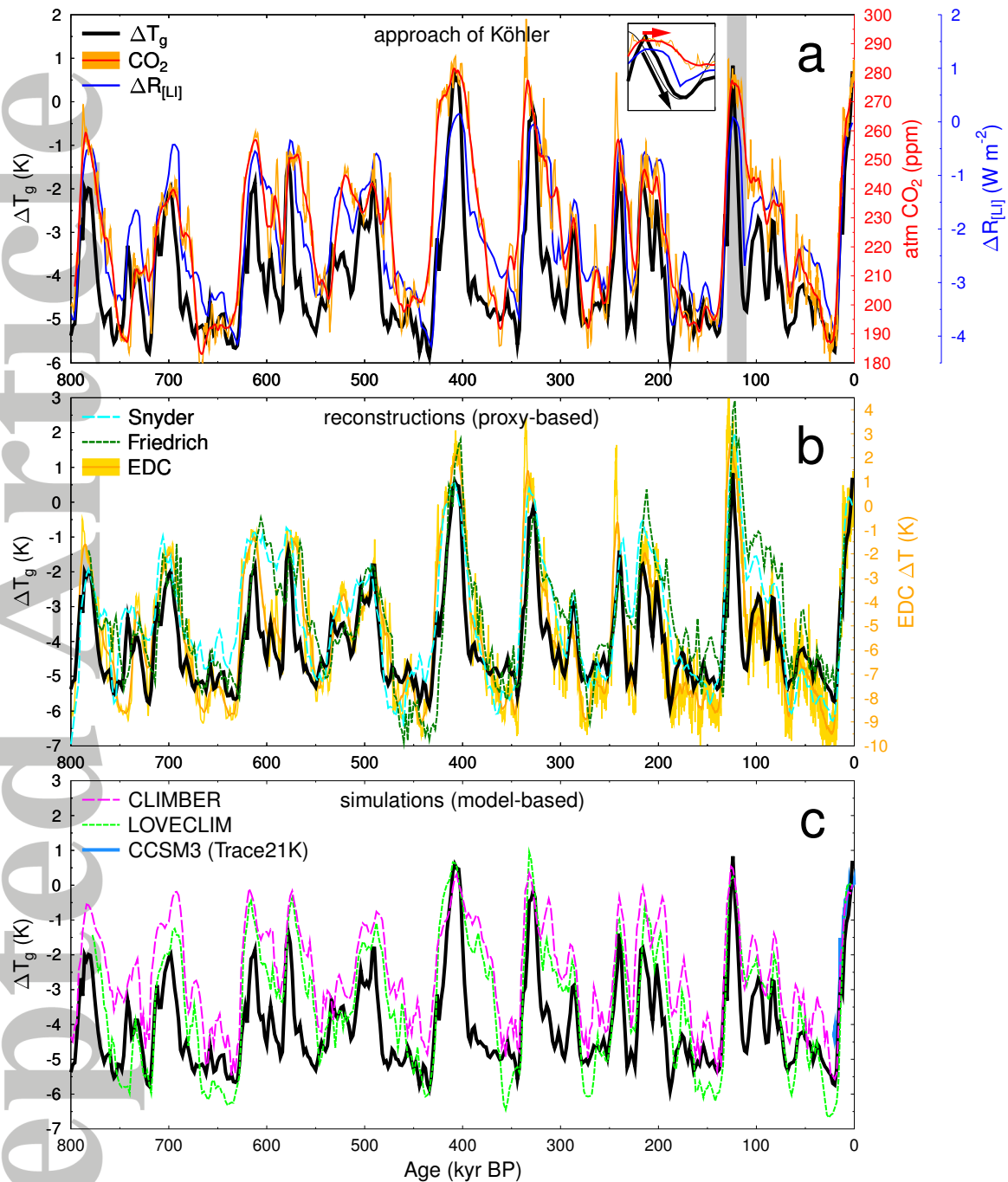


**Figure 1.** Paleodata of the last 800 kyr. (a) Data used in the approach of Köhler (K2015) with global mean temperature change  $\Delta T_g$ , land ice-based radiative forcing change  $\Delta R_{[LI]}$  and atmospheric  $\text{CO}_2$  [Bereiter et al., 2015]. Inset shows an enlarged view on the divergence of  $\Delta T_g$  and  $\text{CO}_2$  at the end of the Eemian (130-110 kyr BP, gray band), including as thin black line changes in obliquity [Laskar et al., 2004]. Comparing different temperature time series with K2015- $\Delta T_g$  (black bold line); (b) proxy-based reconstructions of  $\Delta T_g$  (Synder, Friedrich (F2016)) and EPICA Dome C (EDC)  $\Delta T$ ; (c) model-based simulations (CLIMBER, LOVECLIM) including CCSM3 for the last 21 kyr. Ice core data (EDC  $\Delta T$ ,  $\text{CO}_2$ ) are plotted on the most recent age model AICC2012 [Bazin et al., 2013; Veres et al., 2013] and shown as original high resolution data (thin) and 8-kyr running means (bold).

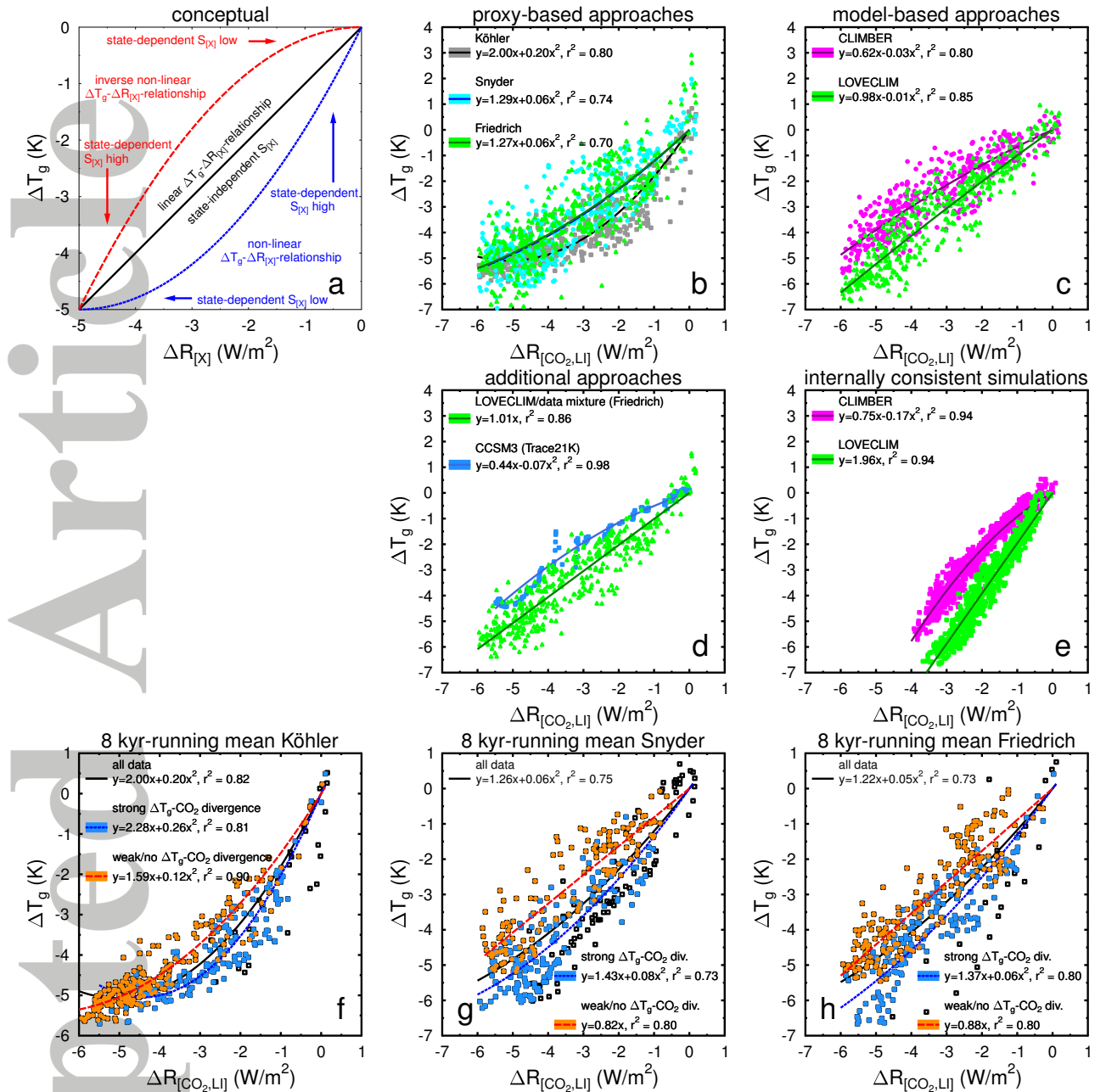


**Figure 2.** Scatter-plots of temperature change  $\Delta T_g$  over radiative forcing change  $\Delta R_{[X]}$ . (a) Conceptual understanding of different relationships between  $\Delta T_g$  and  $\Delta R_{[X]}$  and the resulting state-(in)dependency of  $S_{[X]}$ . (b) data-based reconstructions of  $\Delta T_g$  (Köhler, Snyder, Friedrich); (c) model simulation results of  $\Delta T_g$  (CLIMBER, LOVECLIM); (d) alternative approaches (Friedrich's model/data mixture for  $\Delta T_g$ , 21 kyr transient simulations with CCSM); (e) internally consistent model-setups of CLIMBER and LOVECLIM; (f-h) multi-millennial component (8-kyr running mean) of the proxy-based approaches (f: Köhler; g: Snyder; h: Friedrich) split in time windows with strong or weak divergence of  $\Delta T_g$  and  $CO_2$ . Data are split by the zero line in the standardized ratio  $\Delta T_g/\Delta R_{[CO_2]}$  shown in Fig. 3b. White squares are data points which are filtered out in the standardizing of the data, and therefore neither considered in strong or weak divergence part, but which contribute to the fit through all data. In most plots the same  $\Delta R_{[CO_2,LI]}$  from K2015 is plotted, while in (d) CCSM3 is based on  $\Delta R_{[LI]}$  from ICE-5G; in (e) we show  $\Delta R_{[CO_2,LI]}$  as used in CLIMBER and LOVECLIM.

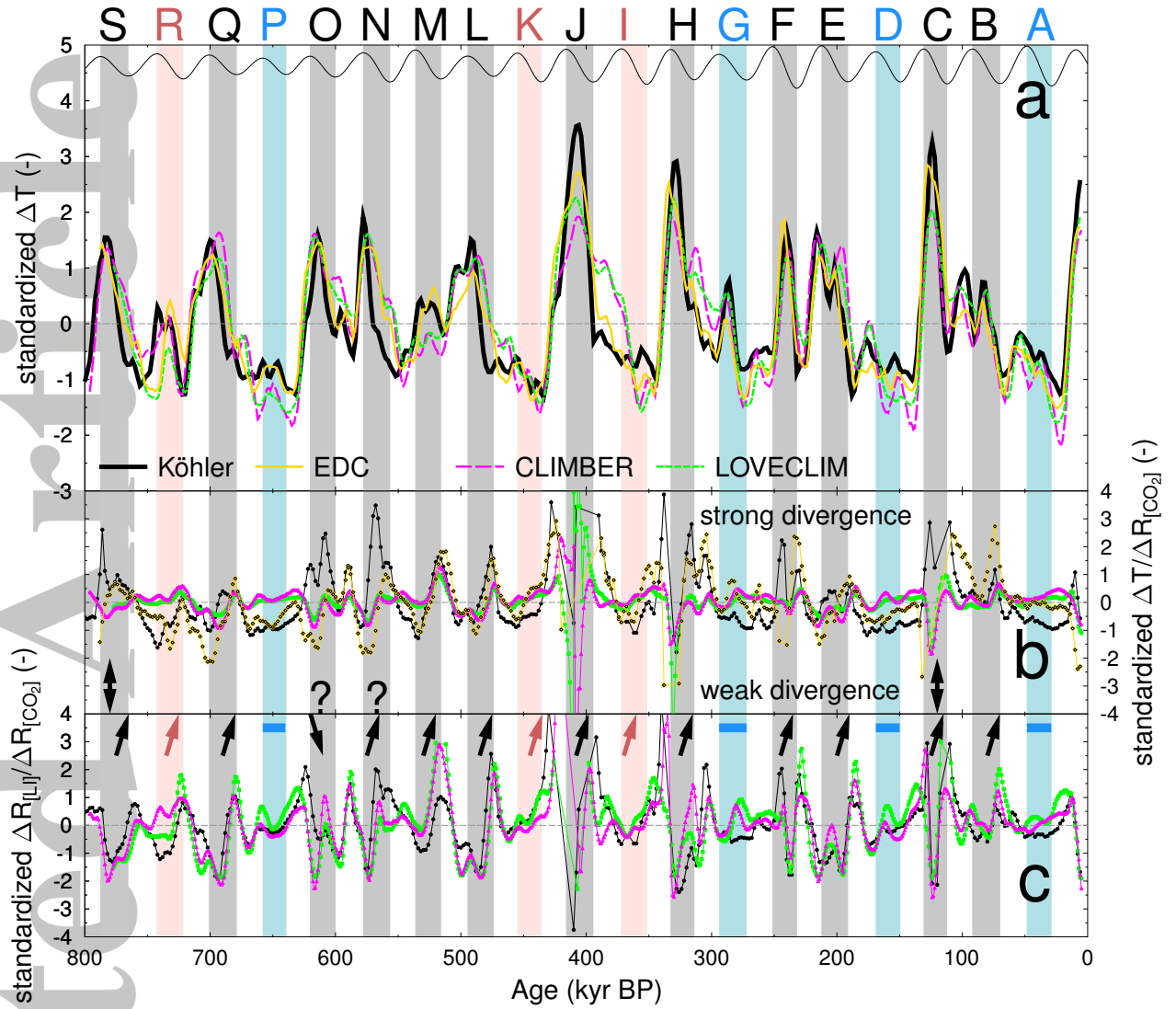


**Figure 3.** Multi-millennial (all data as 8-kyr running mean)  $\Delta T$ - $\text{CO}_2$  divergence and relative contributions of radiative forcing of land ice albedo and  $\text{CO}_2$  for  $\Delta T$  in different setups. (a)  $\Delta T$  (local  $\Delta T$  for EDC and  $\Delta T_g$  elsewhere); (b) the divergence of  $\Delta T$  and  $\text{CO}_2$  described by  $\Delta T/\Delta R_{[\text{CO}_2]}$ ; (c)  $\Delta R_{[\text{LI}]}/\Delta R_{[\text{CO}_2]}$ : relative land ice (sea level) contribution with respect to  $\text{CO}_2$ . The data sets Köhler and EDC differ only by their  $\Delta T$ . From the model simulations (CLIMBER, LOVECLIM) we analyzed the internally used radiative forcing. All data sets have been standardized and outliers in the ratios have been filtered out. Obliquity [Laskar et al., 2004] is sketched on top of sub-panel a (thin black line), with shadings and labels (A–S) indicating times of decreasing obliquity. Color-code is given by the details of the Köhler data-set: gray: strong  $\Delta T_g$ - $\text{CO}_2$  divergence including large variations in relative sea level contribution; light red: no or weak  $\Delta T_g$ - $\text{CO}_2$  divergence and large variations in relative sea level contribution; light blue: no or weak  $\Delta T_g$ - $\text{CO}_2$  divergence and stable relative sea level contribution. Vertical two-headed arrows in the  $\Delta T_g$ - $\text{CO}_2$  divergence panel indicate the anti-phase dynamics partially seen between Köhler and the CLIMBER/LOVECLIM data sets. Question marks in (b) highlight two phases (MIS 15a, MIS15e) during which Köhler and EDC largely disagree.